24th INTERNATIONAL CONGRESS ON SOUND AND VIBRATION
23–27 July 2017, London

ANALYSIS OF FREQUENCY LOCI VEERING PHENOMENA IN DETUNED SPHERICAL RETICULATED SHELL

Zhan-hui Liu*, Ming Zhang, Ke-yue Zhang

Southwest Jiaotong University, School of Civil Engineering, Leshan, China

email: liuzhanhui@swjtu.edu.cn

Wei Liu, Wei-cheng Gao

Harbin Institute of Technology, School of Astronautics, Harbin, China

The frequency loci veering phenomena of spherical reticulated shells are firstly studied by introducing random detuning parameters with normal distribution into the structural stiffness distribution of radial members and latitudinal members respectively. The finite element method is applied to analyze the influences of two assumed detuning patterns on natural frequencies systematically. It is found that the frequency loci veering phenomenon does occur between some typical detuning cases by the 1st detuning pattern. Then, the Frequency Curvature Coefficient $Curv_i$ is proposed to determine the position of veering points. Furthermore, The detuning effects induced by the 2nd detuning pattern, especially the frequency loci veering phenomena are also numerically analyzed for the reticulated shell. It is revealed through numerical simulation that the structural detuning could cause the frequency loci veering and the exact position of veering point can be judged by $Curv_i$.

Keywords: Reticulated Shell, detuning, Frequency Loci Veering, Frequency Curvature Coefficient

1. Introduction

In practical engineering, the perfect structure is almost nonexistent. Owning to the manufacturing or construction errors, geometrical irregularity, material defects and structural damage, etc., the imperfections of the structure are inevitable. Imperfection is also called “detuning” and correspondingly the structure with imperfection is called a “detuned” structure. Over the past several decades, many researchers studied the curve veering phenomenon for the detuned structures. As early as 1962, Claassen [1] reported that some interesting phenomenon appeared in the transverse vibration analysis of a thin rectangular cantilever plate. In fact, the “avoid crossing” of frequency loci mentioned by Claassen is just the curve veering phenomenon. In 1974, Leissa [2] pointed out that the curve veering phenomenon might be an aberration induced by the approximation method--Galerkin method in the study on the transverse vibration of rectangular membrane. But, in 1981, after investigating the same example taken by Leissa, Kuttler verified that curve veering could be an actual phenomenon and was not always caused by the approximation techniques [3]. Schajer [4], Perkins and Mote [5] also verified the existence of the curve veering in both the approximate and exact solutions associated with the vibration of a rotating circular string, respectively. Later, Gottlieb [6], together with Perkins and Mote [7], discussed the curve veering of a coupled pendulum and a coupled oscillator, emphasized the importance of the coupling to the veering process, and clarified the differences between the vibrations of two structures. In other literatures, the curve veering phenom-

enon was studied in more and more complex structures, such as three-dimensional, cyclically symmetric CPVAs (Centrifugal pendulum vibration absorbers) [8], weakly coupled double beam system [9], detuned blade disks [10], pretwisted rotating compressor blade [11], rolling tyre [12], rotating rectangular thin plate [13], cable-stayed and suspension bridges[14], and so on.

It is clear from the foregoing that the structural detuning may significantly affect the vibrational modal properties of the structure, such as the frequency loci veering phenomena may occur; the phenomena closely depends on the continuous variation of some structural detuning parameters; and these researches of frequency loci veering mainly focused on periodic structures or symmetrical structures. As one of the periodic structures with cyclic symmetry, spherical reticulated shell structures also consist of many identical or similar member bars; however, to our knowledge, little work has been devoted to the analysis of the frequency loci veering in these architecture structures with many applications. As mentioned above, the imperfections of the structure are inevitable. If we ignore the detuned-effect and still analyze the dynamic behaviour of the detuned structure based on the structural frequencies characteristics of the tuned structure, it might cause inaccurate or even completely erroneous conclusion on the parameter identification and structural health monitoring. Therefore, it is necessary to investigate the frequency loci veering of reticulated shell. In this study, the motivation is to verify if the reticulated shell structure has similar frequency loci veering behavior by the FEA method. Moreover, this paper is also to pursue a method for determining the position of veering points.

The main research work in this study includes: (1) A number of studies on the curve veering phenomenon are reviewed; (2) the FEA model of a single-layer spherical reticulated shell is established. The natural frequency characteristics of the tuned reticulated shell are analyzed; (3) the frequency loci veering phenomenon for two detuning patterns is studied and the characteristics of frequency loci veering in the spherical reticulated shell are discussed.

2. Frequency characteristics Analysis of tuned reticulated shell

2.1 Analytical model

As shown in Figure 1, a single-layer spherical reticulated shell consists of radial members and latitudinal members. The span and rise-span ratio are 30m and 1/4.4, respectively. All the members are steel circular pipes with the cross-section sizes: Φ180×12 for radial members and Φ108×4.5 for latitudinal members. The material of members is Q345 steel with the density of 7850kg/m^3, the Young's modulus of 206GPa and the Poisson's ratio of 0.3. The uniformly distributed vertical load of the roof is 60kg/m^2. Because it is difficult to achieve an exact analytical solution for this kind of large and complex structures, the powerful FEA technique is used to analyze the modal properties of the reticulated shell.

In the FEA model, all the members are assumed to rigidly be connected at nodes and treated as Beam188 elements. The Beam 188 element is two-node beam element in 3-D defined in ANSYS and based on the beam theory of Timoshenko which includes shear-deformation effects. The vertical load of the roof is converted to lumped masses at the nodes of the reticulated shell and then the lumped masses are simulated by using the MASS21 element. The self-weight of the structure is applied and solved with the help of macro file compiled in APDL of FEM software ANSYS. All the nodes at the fourth ring are assumed to be fixed, as marked in Figure 1.

In order to facilitate the following description, all the radial members are divided into 24 groups and numbered in Figure 1. Each group consists of 6 radial members. All the latitudinal members are also divided into 24 groups, for example, the 1st group of latitudinal members denotes all the latitudinal members between the 1st and 2nd groups of radial members; the 2nd group of latitudinal members denotes the latitudinal members between the 2nd and 3rd groups of radial members and so on.

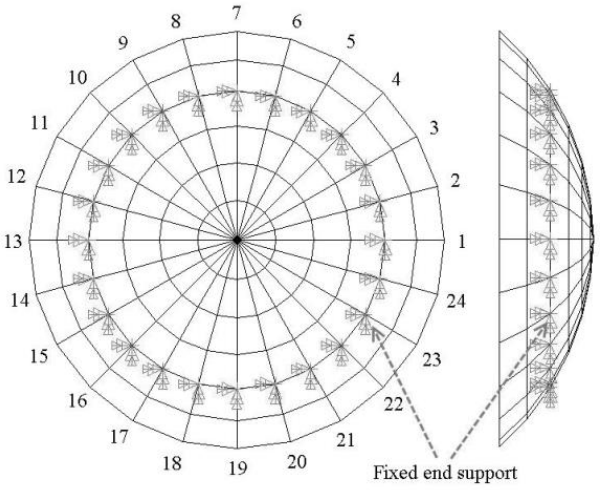

Figure 1. Analytical model of reticulated shell

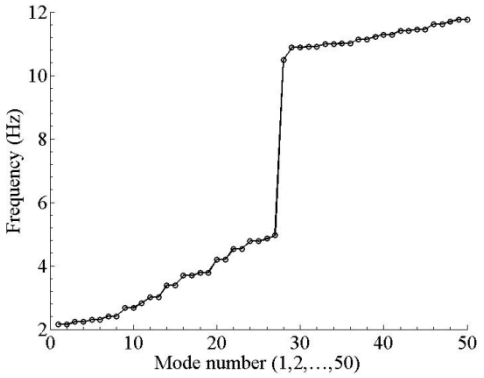

Figure 2. Natural frequencies of tuned structure

2.2 Frequency characteristics of tuned structure

Using the FEA software ANSYS, the first 50 natural frequencies are extracted with the Block Lanczos Method from the tuned reticulated shell in Figure 1. From the curve in Figure 2, it can be seen that: (1) the frequencies of the tuned structure are divided into two typical frequency bands. The 1st frequency band (from the 1st frequency to the 27th frequency) and the 2nd frequency band (from the 28th frequency to the 50th frequency) are distributed on the open interval (0, 5) and the open interval (10, 12), respectively. The 2nd frequency band is more intensive than the 1st frequency band. (2) The reticulated shell structure has very high modal densities. Because of the symmetrical properties of the tuned structure, there are repetitive frequency features in the first 50 natural frequencies.

Previous studies show that the structural detuning destroys the regular feature of the mode and might lead to the occurrence of frequency loci veering phenomenon. Undoubtedly, it will lead to completely erroneous results in analyzing the detuned structure based on the structural dynamic properties of the tuned structure. Therefore, it is essential to investigate how the presence of detuning affects the frequencies characteristics of the structure.

3. Random numbers and detuning patterns

3.1 Generation of random numbers

The distribution of detuning parameters is random actually, so how to generate random number is crucial for an accurate analysis of the detuning-induced effect. It should be pointed that random numbers produced by software are not random in a strict mathematical sense [15]. In other words, they are pseudo-random and pseudo-independent. However, software applications, such as MATLAB, use algorithms that make the results pass various statistical tests of randomness and independence. Hence, we can use these numbers as if they are truly random and independent. One benefit of using pseudo-random numbers is that one can repeat a random number calculation at any time. This can be used to generate the detuning parameters with the same form in the distribution and different standard deviation by specifying the same generator and seed type together.

The detuning ratio ε is introduced into the structure by generating sample size 24 from a normal distribution with the mean 0 and the standard deviation σ. ε represents the ratio between the detuning and ideal parameters, and reflects the detuning level. Different detuning cases correspond to the ε samples with different σ. The limit of σ is varied from 0.0025 to 0.3200 with a step $\Delta\sigma$ =0.0025, so there are 128 detuning cases. Some typical detuning distribution patterns of ε are shown in Figure 3.

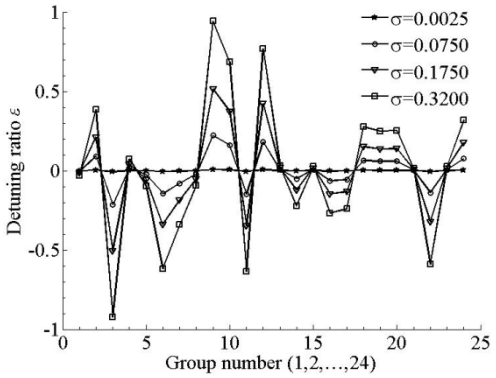

Figure 3. Detuning distribution patterns

3.2 Detuning patterns

The analyses of two different detuning patterns, stiffness detuning pattern of radial members, and stiffness detuning pattern of latitudinal members, are carried out to reveal the detuning-induced effect on the frequency loci of the spherical reticulated shell.

Detuning pattern 1: the detuning is introduced into the 24 groups of radial members by altering their stiffness with ε.

Detuning pattern 2: in the same manner as the 1st detuning pattern, the stiffness detuning is introduced into the 24 groups of latitudinal members by ε.

It is worth noting that $\sigma = 0$ represents the tuned case. 128 detuning cases and one tuned case have been calculated for each detuning pattern.

4. Frequency loci veering behavior of two detuning pattern

4.1 Frequency loci veering of the 1st detuning pattern

The detuning effect induced by the 1st detuning pattern, especially frequency loci veering characteristics, is numerically analyzed for the reticulated shell in Figure 1. The first 50 natural frequencies for the 128 detuning cases corresponding to the 1st detuning pattern and one tuned case are extracted from the FEA data of the spherical reticulated shell. Figure 4 shows the relationship between the frequencies 1-16 and the standard deviation of detuning parameters σ in succession from the bottom upward, in which the alternation of solid and dotted lines represents the difference of two adjacent frequency loci. There are pairs of vibration modes with the same frequency when $\sigma = 0$, but the locus of the same frequency then disperse in two different directions which indicates that the detuning damages the symmetry properties of the tuned structure and the multiplicity disappears.

Figure 4 shows that the loci of frequencies 1-16 versus σ do not violently, but after the 16th frequency, some interesting phenomenon occurs as shown in Figure 5. As σ increases, the 17th and 18th frequency loci first approach each other and almost intersect at the region R, then rapidly diverge like taking the previous path of the other, respectively. Obviously, the curve veering phenomenon of frequency loci occurs in the region R. The difference between the two frequencies has the minimum value 8.621×10^{-5} Hz when $\sigma = 0.2975$, only about 0.002% of the 17th frequency value. In addition, the 18th and 19th frequencies are the same when $\sigma = 0$, but they are then divided into two branches, which also signifies that the symmetry of the tuned structure is destroyed and the modes with the same frequency become the modes with distinct frequencies.

In order to describe the frequency loci veering phenomenon, the Frequency Curvature Coefficient (Eq. 1) is proposed to calculate the curvature of the frequency locus

$$Curv_i = \frac{|\omega_i''|}{\left(1+\omega_i'^2\right)^{3/2}}. \quad (1)$$

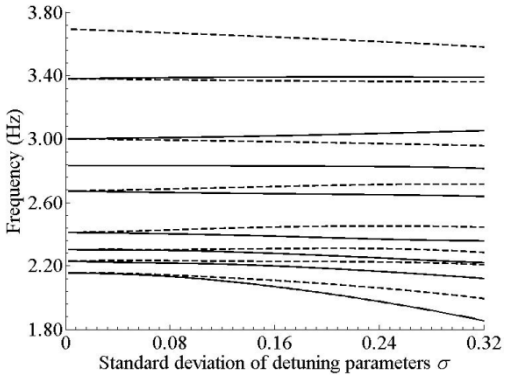

Figure 4. Loci of frequencies 1-16 versus σ

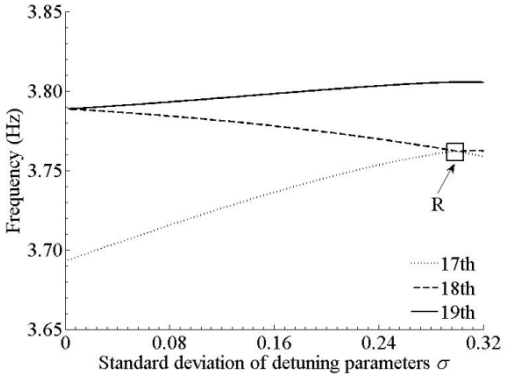

Figure 5. Loci of frequencies 17-19 versus σ

where $Curv_i$ represents the curvature of the ith frequency locus; ω_i' and ω'' are the first-order derivative and the second-order derivative of the ith frequency locus versus σ, respectively. It needs to note that the MATLAB built-in routine "*gradient*()" and "*del2*()" are used to calculate ω_i' and ω'' through computing a single-sided difference at the end data points and a central difference at the interior data points respectively, which can return an array with the same number of elements as the input data.

Figure 6 displays the curvature variation of frequencies 1-17. It can be seen that the curvature of the 17th frequency locus significantly increases in magnitude and has a peak at the position of $\sigma = 0.2975$, while others have not peaks. It needs to indicate that X is σ value and Y is the curvature value at the peak corresponding to the veering region L in Figure 6. Figure 7 shows that the variation in the curvature plot of the 18th frequency locus; it also has a peak at the position of $\sigma = 0.2975$. The peak values of curvature plot in Figures 6 and 7 are 72.89 and 68.09, respectively. The position of veering points is very clear in the $Curv_i$ variation of frequency loci.

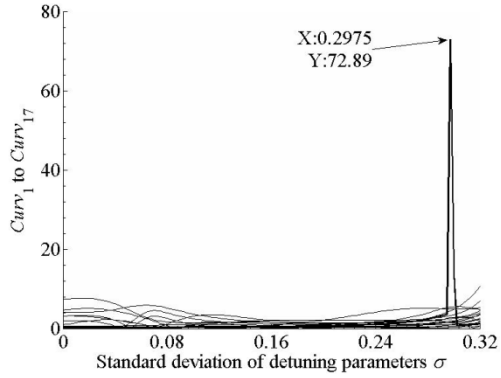

Figure 6. Curvature of 1-17th frequency loci

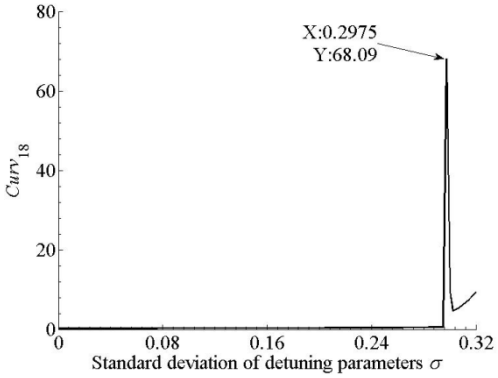

Figure 7. Curvature of 18th frequency locus

Except the 17th and 18th frequencies, the 26th and 27th frequencies also present the frequency loci veering phenomenon. At $\sigma = 0.3100$, the 26th and 27th frequency loci do not cross but their frequencies, 4.909272Hz and 4.910236 Hz, are quite close indeed (not shown here for brevity). Therefore, two pairs of frequency loci (the 17th and 18th frequencies, the 26th and 27th frequencies) present the curve veering phenomena within the 1st frequency band of the tuned reticulated shell in Figure 2. The exact position of veering point can be judged by the $Curv_i$ variation of the frequency locus.

Similarly, Figure 8 shows the variation of frequencies 32-40 versus σ. It presents an interesting feature that the curve veering phenomenon presents in more than one region for the same frequency

locus. For example, the 37th frequencu locus has 5 veering regions with the two adjacent frequency loci. Statistical data demonstrates that the numbers of veering regions corresponding to the 1st and 2nd frequency bands are 2 and 31 respectively. It can be seen that the more intensive the modes are, the more possible the frequency loci veering would be. Also, the exact position of veering points can be determined by the peak position of the curvature variation of frequency loci.

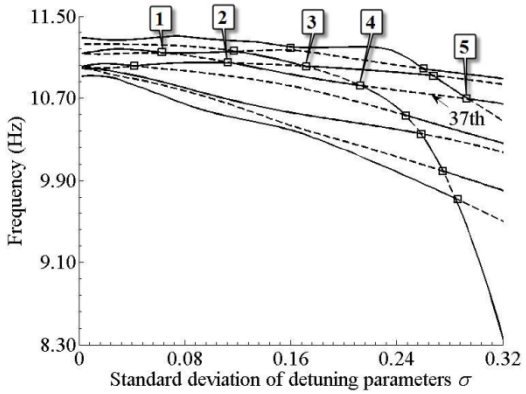

Figure 8. Loci of frequencies 32-40 versus σ

4.2 Frequency loci veering of the 2nd detuning pattern

The detuning effects induced by the 2nd detuning pattern, especially the frequency loci veering phenomena are also numerically analyzed for the reticulated shell. The first 50 natural frequencies for the 128 detuning cases corresponding to the 2nd detuning pattern and one tuned case are also extracted from the FEA data of the spherical reticulated shell. Loci characteristics of varying stiffness of latitudinal members are discussed in this section too. Since the frequency loci do not violently change before the 16th frequency, the 4 loci of frequencies 16-19 versus σ are shown only for a representative instance in Figure 9. Evidently, the 16-19th frequency loci also present the veering phenomena.

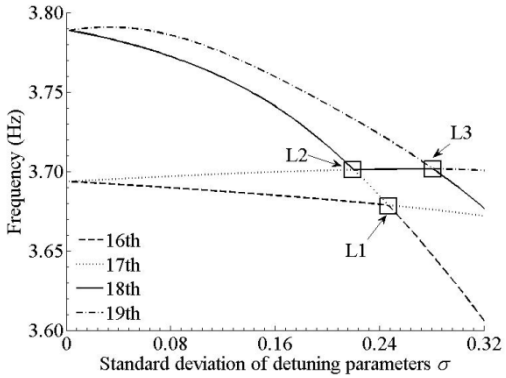

Figure 9. Loci of frequencies 16-19 versus σ

It can be seen from Figure 9 that there are 3 veering regions marked as L1, L2 and L3. The 16th frequency locus veers away from the 17th frequency locus in the veering region L1. Correspondingly, there is a peak 149.2 on the curvature variation of the 16th frequency at the position $\sigma = 0.2450$ as shown in Figure 10. Similarly, the 17th frequency locus veers away from the 16th and 18th frequency loci in two veering regions L1 and L2, respectively; correspondingly, the curvature variation of the 17th frequency has two peaks 248.9 and 190.9 at the position $\sigma = 0.2450$ and $\sigma = 0.2175$ in Figure 11. At $\sigma = 0.2450$, the 16th and 17th frequencies are 3.678148 Hz and 3.678699 Hz respectively. It is clear that the position of veering points can be judged by the peak position of curvature variation and the pair of frequencies in the same veering region L1 are quite close. The analyses of the 18th and 19th frequency loci are the same as that of the 16th and 17th frequency loci, so their description will not repeat again.

Figure 12 shows the variation of frequencies 31-39 versus σ. Besides, the similar feature that the curve veering phenomenon occurs in more than one region for the same frequency locus, is also found in both the 1st and 2nd frequency bands for the 2nd detuning pattern, such as the 17th and 18th frequency loci (Figure 9) for the 1st frequency band and the 38th frequency locus (Figure 12) for the 2nd

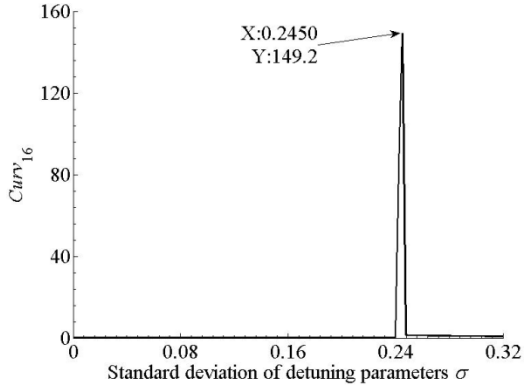

Figure 10. Curvature of 16th frequency locus

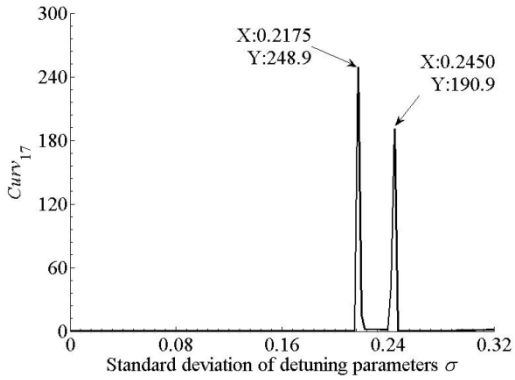

Figure 11. Curvature of 17th frequency locus

frequency band. Statistical data demonstrates that there are 5 and 15 veering regions within the 1st and 2nd frequency bands, respectively. The number of veering regions in the 2nd frequency band is more than that in the 1st frequency band. This is consistent with the conclusion of the 1st detuning pattern. Also, the exact position of veering points can be judged by the peak position of the $Curv_i$ variation of frequency loci.

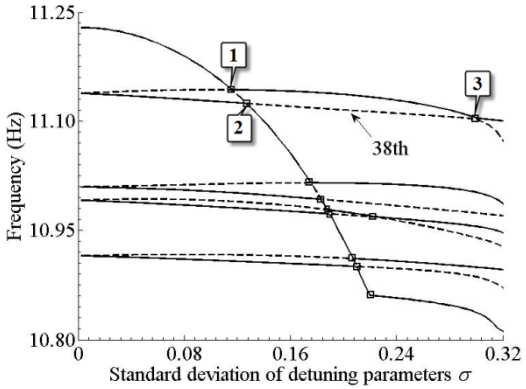

Figure 12. Loci of frequencies 31-39 versus σ

5. Concluding remarks

Study on structural frequency loci veering phenomena is extended to the long-span space structure--reticulated shell. In this paper, the FEM simulations and dynamic analysis are applied to investigate the effect of variation in structural parameters on the phenomena; in addition, two detuning patterns of stiffness and mass are proposed to reflect the configuration feature of the shell structure. The conclusions can be given as follows:

1) The numerical simulation verifies that the frequency loci veering does occur between some particular detuning cases of single-layer spherical reticulated shell structure, for the two assumed detuning patterns of stiffness.

2) One method using the curvature of frequency loci is proposed to judge the exact position of frequency loci veering.

3) The possibility of the frequency loci veering is closely related to the intensity of modes.

4) The potential influence of the curve veering phenomena on the parameter identification and structural health monitoring should be paid enough attention for civil engineering structures like reticulated shell.

6. Acknowledgments

The authors wish to express their sincere thanks to Professor Guang-chun Zhou of Harbin Institute of Technology for his valuable discussions and comments on the manuscript. And this research is supported by the National Natural Science Foundation of China (Grant No. 51108128), the Scientific Research Projects for Building High-level Faculty in Southwest Jiao tong University (Grant No. 10101X10096077) and the Science and Technology Innovation Project for the Central Universities (Grant No. 10101B10096043). Such financial aids are also gratefully acknowledged.

REFERENCES

1 Claassen, R. W. Vibrations of a rectangular cantilever plate, *Journal of the Aerospace Sciences*, 11 (29), 1300–1305, (1962).

2 Leissa, A. W. On a curve veering aberration, *Journal of Applied Mathematics and Physics (ZAMP)*, 25 (1), 99-111, (1974).

3 Kuttler, J. R. On curve veering, *Journal of Sound and Vibration*, 75(4), 585-588, (1981).

4 Schajer, G. S. The vibration of a rotating circular string subject to a fixed elastic restraint, *Journal of Sound and Vibration*, 92 (1), 11-19, (1984).

5 Perkins, N. C., Mote, C. D. Comments on curve veering in eigenvalue problems, *Journal of Sound and Vibration*, 106 (3), 451-463, (1986).

6 Gottlieb, H. P. W. Extension of a text-book problem to curve veering for coupled pendulums, *Journal of Sound and Vibration*, 113(1), 185-187, (1987).

7 Perkins, N. C., Mote, C. D. Extension of a text-book problem to curve veering for coupled pendulums-reply, *Journal of Sound and Vibration*, 113 (1), 188-189, (1987).

8 Shi, C.Z., Parker, R.G. Vibration modes and natural frequency veering in three-dimensional, cyclically symmetric centrifugal pendulum vibration absorber systems, *ASME Journal of Vibration and Acoustics*, 136 (1), 011014, (2013).

9 Huang, M., Liu, J. K. Substructural method for vibration analysis of the elastically connected double-beam system, *Advances in Structural Engineering*, 16 (2), 365-377, (2013).

10 Klauke, T., Strehlau, U., and Kuehhorn, A. Integer frequency veering of mistuned blade integrated disks, *ASME Journal of Turbomachinery*, 135 (6), 061004, (2013).

11 Sun, J., Arteaga, I. L., and Kari, L. General shell model for a rotating pretwisted blade, *Journal of Sound and Vibration*, 332 (22), 5804-5820, (2013)

12 Kozhevnikov, I. F.Vibrations of a rolling tyre, *Journal of Sound and Vibration*, 331 (7), 1669-1685, (2012).

13 Zhao, J., Tian, Q., and Hu, H.Y. Modal analysis of a rotating thin plate via absolute nodal coordinate formulation, *Journal of Computational and Nonlinear Dynamics*, 6 (4), 041013, (2011).

14 Chen, X.Z., Kareem, A. Curve veering of eigenvalue loci of bridges with aeroelastic effects, Journal of Engineering Mechanics, 129 (2), 146-159, (2003).

15 Yang, W. Y., Cao, W.W. , Chung, T.S., and Morris, J. *Applied Numerical Methods Using MATLAB*, John Wiley & Sons, Hoboken, NJ (2005).